A Newly Defined m7G-Related Gene Signature for Overall Survival Prognosis of Kidney Renal Clear Cell Carcinoma

Lebin Yuan
The Second Affiliated Hospital of Nanchang University
Fei Cheng
The Second Affiliated Hospital of Nanchang University
Zhao Wu
The Second Affiliated Hospital of Nanchang University
Wei Shen (shenweiniu@163.com)
The Second Affiliated Hospital of Nanchang University

Research Article

Keywords: kidney renal clear cell carcinoma, m7G methylation, overall survival, gene biomarkers

Posted Date: March 7th, 2022

DOI: https://doi.org/10.21203/rs.3.rs-1415171/v1

Abstract

Background: Kidney renal clear cell carcinoma (KIRC) is a highly malignant disease with unsatisfactory prognosis. In recent years, it has been reported that m7G methylation can regulate promoter sequence and induce gene expression or silencing so that affect tumor progression. However, the prognostic value of m7G-related genes in KIRC needs to be further clarified.

Methods: In this paper, we downloaded the mRNA expression profile and corresponding clinical data of KIRC patients from the public database TCGA. The least absolute shrinkage and selection operator (LASSO) Cox regression model was utilized to construct a multigene signature in the TCGA cohort. A risk score model was established based on Kaplan-Meier and multivariate Cox regression analysis. Then, we performed functional enrichment analysis and immune infiltration analysis of differentially expressed genes between high-risk group and low-risk group.

Result: 13 differentially expressed genes (DEGs) were found in normal and tumor tissues. Based on the median score calculated by the risk score formula from 29 m7G-related genes, 534 patients were divided into low-risk and high-risk subgroups, respectively. The survival probability of KIRC patients in the low-risk group was significantly better than that in the high-risk group($p<0.001$). The tumor grade and risk level were independent predictors for OS in multivariate Cox regression analyses ($HR> 1$, $P< 0.01$). Receiver operating characteristic (ROC) curve analysis confirmed the signature's predictive capacity. Functional analysis revealed that human immunodeficiency was enriched, and immune status were different between two risk groups.

Conclusion: A new m7G-related gene biomarker can be used to predict the prognosis of KIRC, which may be a therapeutic option for KIRC patients.

Introduction

Kidney renal clear cell carcinoma (KIRC) accounts for 80% of renal malignant tumors and is one of the most common malignant tumors in the world[1]. Surgical resection is still the main treatment for most KIRC patients, which have improved the short-term survival rate of KIRC to a certain extent. 30% – 40% of patients with localized diseases had metastasis and recurrence during follow-up after surgical resection [2]. The recently proposed cytoreductive therapy has been questioned[3]. Historically, KIRC is one of the earliest malignant tumors that respond to immunotherapy and one of the most sensitive tumors[4], but the result is not satisfactory. Therefore, more treatments need to be explored.

Methylation is an important epigenetic mechanism, which involves many basic biological processes[5], which is usually a marker gene of transcriptional activity. It can be expressed as oncogene or tumor suppressor gene, resulting in different biological phenotypes. Recently, it has been reported that m6A modified long noncoding RNA has diagnostic and prognostic value in renal clear cell carcinoma[6]. Xu et al. Studied the important role of m6A modification and METTL14/BPTF axis in KIRC epigenetics and metabolism, suggesting that methylation plays an important role[7]. The study of biomarkers will help us

to further explore the pathogenesis of KIRC disease and provide new diagnosis and treatment strategies. M7G RNA methylation (N7 methyladenosine, m7G) is a modification in which methyl is added to the seventh position N of RNA guanine (g) under the action of methyltransferase. M7G modification is one of the most common forms of base modification in post transcriptional regulation. It is widely distributed in tRNA, rRNA and 5 hats of eukaryotic mRNA, and plays an important role in maintaining RNA's processing, metabolism, stability, nucleation and protein translation[8]. However, the relationship between these m7G related genes and the prognosis of KIRC patients remains unclear.

In this study, we downloaded the mRNA expression profile and corresponding clinical data of KIRC patients from the public database, Then, we constructed a polygenic marker with m7G-related differentially expressed genes (DEGs) in the TCGA cohort. Finally, we further conduct relevant functional analysis to explore the potential mechanism. By analyzing differentially expressed genes with m7G, we carried out a new research perspective to understand the role of m7G in the development of KIRC in more detail and determine the reliable prognostic predictors of KIRC patients.

Materials And Methods

The flow chart of this study is shown in Fig. 1. After removing the data without survival time data, we obtained 533 survival related TCGA-KIRC clinical data. Table 1 summarizes the detailed clinical characteristics of these patients.

Table 1
Clinical characteristics of KIRC patients used in this study

characteristics	TCGA cohort	percentage
Total number of patients	537	
Age (median, range)	60.59(26–90)	
Sex		
Female	191	35.60%
Male	346	64.40%
Status		
Die	177	33%
Live	360	67%
Survival time		
OS days(median)	1334	
Grade		
G1	14	2.60%
G2	229	42.60%
G3	208	38.70%
G4	78	14.50%
unknown	8	1.60%
Stage		
I	269	
II	57	50.10%
III	125	23.30%
IV	83	15.50%
unknown	3	11.10%
T stage		
T1	275	51.20%
T2	69	12.80%
T3	182	33.90%
T4	11	2.10%

characteristics	TCGA cohort	percentage
N stage		
N0	240	44.70%
N1	17	3.20%
unknown	280	52.10%
M stage		
M0	426	79.30%
M1	79	14.70%
unknown	32	6%

Table 2
Baseline characteristics of patients in different risk groups

Clinicopathological features	content	low risk	high risk	P
Age(year)	< 60	46	57	0.5178
	>=60	70	72	
Sex	Female	47	49	0.6963
	Male	69	80	
Grade	G1 + G2	55	53	0.3674
	G3 + G4	61	76	
Stage	I + II	68	48	0.1613
	III + IV	64	65	
T	T1 + T2	72	72	0.3635
	T3 + T4	44	57	
M	M0	101	103	0.17
	M1	15	26	
N	N0	112	119	0.1757
	N1	4	10	

Data Collection from TCGA

The gene expression profiles of KIRC were downloaded from TCGA (https://portal.gdc.cancer.gov/). In the TCGA database, all data on KIRC and corresponding clinical information were freely downloaded by

TCGA GDC Data portal[9]. There were 611 COAD samples, including 539 tumor and 72 normal tissues. The gene expression profile was standardized using the scale method provided in the "limma" R software package. Using standardization to read the count value. On the other hand, 29 m7G-related genes were retrieved from previous literature[8] and provided in supplementary table S1.

Obtain of m7G-related Risk Genes and Construction of Prognosis Related Model

In TCGA cohort, EdgR (version 3.32.1) and limma[10] (version 3.36.0) software packages in Bioconductor were used to process data with false discovery rate (FDR) < 0.05, a total of 21 DEGs genes were obtained. At the same time, we downloaded the clinical data of TCGA-KIRC and removed useless data. Based on DEGs and survival related data, the forest map was drawn by forestplot package with adjust P < 0.1 in R, a total of 18 prognostic genes were obtained. The VennDiagram[11] package in R had been installed to plot the Venn diagram to visualize the consequences of the intersection between DEGs and 18 prognostic genes. Finally, by installing pheatmap package and iGraph package in R, we mapped the heat map and correlation analysis of 13 intersection genes.

To effectively identify the m7G-related gene modules, we first adopt LASSO Cox regression model by R package “glmnet” and “survival”[12], a total of 9 genes were obtained and we also drew the forest map based on P < 0.05. Next, risk score was performed. The risk score is calculated by the "scale" function of R in TCGA data. Then, KIRC patients were divided into high-risk group and low-risk group based on median risk score, and the Kaplan–Meier analysis of OS time, 1,2,3-year ROC curve, PCA and t-SNE was performed after installed “Rtsne”, “timeROC” and “survival” package in R. The "bioRiskPlot " function based on risk score shows the distribution and survival status of patients.

Independent prognostic analysis of risk score

We obtained the clinical data of KIRC patients from the public database TCGA, including age, gender, stage, grade and TNM. Chi-squer Test and Fisher Test was used to study according to the risk score. Moreover, we used univariate and multivariate Cox regression models for analysis. All the above operations are completed in R.

Functional enrichment analysis of DEGs

Before gene function analysis, we divided TCGA-KIRC patients into high-risk and low-risk groups according to the median risk score. Through gene expression files and differential screening of genes in each group (FDR < 0.05 and | log2FC | ≥ 1), 87 differential genes were finally obtained. Based on these DEGs, Gene Ontology (GO) and Kyoto Encyclopedia of Genes and Genomes (KEGG) analysis were performed by R and Online database KOBAS (http://kobas.cbi.pku.edu.cn/kobas3/genelist/). By using “GSVA”, “limma” and “ggpubr” packages in R, ssGSEA was calculated to obtain the score of immune infiltrating cells and evaluate the function of immune related cells and molecules.

Statistical analysis

Single-factor analysis of variance was used to compare gene expression levels, Pearson Chi-square test and Fisher test were used to test categorical variables. Kaplan-Meier analysis and log-rank comparison univariate and multivariate Cox regression were used to determine independent predictors of OS. The Mann-Whitney test was used to compare immune cell infiltration and pathway activation between the two cohorts. All statistical analyses were performed using R software (v3.6.3).

Results

Identification of prognostic m7G-related DEG in TCGA cohort

By comparing the expression levels of 29 m7G-related genes and TCGA-KIRC data of 539 tumors and 72 normal subjects, 21 differentially expressed genes were finally found based on R ($P < 0.05$). Among these genes, 9 genes (NUDT10, NUDT4, EIF4E, NUDT16, NUDT3, DCPS, NCBP1, WDR4, LSM1) were down-regulated and 12 genes (SNUPN, NCBP3, EIF3D, DCP2, METTL1, IFIT5, NSUN2, AGO2, GEMIN5, NCBP2L, NUDT11, EIF4A1) were up-regulated in tumor tissues. By integrating differential genes, we obtained 18 prognosis related genes (DCP2, NCBP2, LSM1, LARP1, NUDT3, WDR4, NUDT10, EIF4E, EIF4E1B, NUDT16, NUDT4, GEMIN5, IFIT5, CYFIP1, EIF4A1, METTL1, EIF4E3, NUDT11) based on adjust $P < 0.1$. Finally, we drew the Venn diagram and obtained 13 intersection genes (Fig. 2A, Fig. 2C), and the correlation between these genes is shown in the Fig. 2B. The 13 prognostic difference genes related to m7G are DCP2, EIF4A1, EIF4E, GEMIN5, IFIT5, LSM1, METTL1, NUDT10, NUDT11, NUDT16, NUDT3, NUDT4, WDR4 respectively(Fig. 3A). The interaction network between these genes is made through the online database STRING(https://cn.string-db.org/)(figure3B).

Development of a Prognostic Gene Model in the TCGA Cohort

Using LASSO Cox regression analysis, a prognostic model was established by using the expression profiles of the above 13 genes, and 9 gene signatures were constructed(Fig. 4A,4B,4C). According to the "scale" function of R in TCGA data, the risk score was calculated and divided into two subgroups based on median risk score, including 265 patients in high-risk group and 269 patients in low-risk group. The Kaplan-Meier curve showed that the OS of patients in the high-risk group was significantly lower than that of patients in the low-risk group after survival package calculation ($P < 0.001$, Fig. 5A). It is suggested that the death probability of high-risk patients is higher than that of low-risk patients. In order to evaluate the specificity and sensitivity of the prognostic model, we used time-dependent ROC to analyze the 1-year, 2-year and 3-year survival rates. The AUCs were 0.672, 0.636 and 0.642, respectively(Fig. 5B). The patients in the high-risk group had more deaths and shorter survival time than those in the low-risk group. Consistently, PCA and t-SNE analysis showed that the distribution of patients in different risk groups tended to move in different directions (Fig. 5C-F).

Independent Prognostic Value of the Risk Model

Univariate and multivariate Cox regression analysis were used to find independent prognostic factors. In Univariate Cox analysis, risk score, risk level, tumor stage, tumor grade, T and M stage were independent prognostic factors, age, gender and N stage were not(Fig. 6A). However, only tumor grade (HR =

1.6658,95% CI = 1.0674 − 2.5996, P = 0.0246) and risk level (HR = 2.4149,95% CI = 1.5176 − 3.8428, P < 0.001) were independent prognostic factor in multivariate Cox regression analysis(Fig. 6B). In addition, we created a Heatmap of clinical characteristics of the TCGA cohort and found significant differences between the two subgroups(Fig. 6C).

Functional analysis based on risk model

Based on the use of limma package in R, we identified 87 differential genes from the previously obtained risk groups and TCGA cohort, including 79 down-regulated genes and 8 up-regulated genes. In this paper, we only get CC in GO, which is mainly concentrated in synaptic membrane(Fig. 7A). Therefore, we further analyze KEGG by KOBAS and find that it is mainly concentrated in human immunodeficiency virus 1 infection(Fig. 7B). The results showed that m7G-related DEGs played an important role in immune function in KIRC. To further explore the correlation between risk score and immune status, we used ssGSEA in R to compare the enrichment fractions of 13 immune related pathways and 16 immune cell activities among different groups in TCGA. Interestingly, contents of the immune response cells, including the score of CD8 T cells, pDCs, Tfh were significantly different between the low risk and high-risk group in the TCGA cohort (all adjusted P < 0.05, Fig. 7C). Moreover, the cytokine-cytokine receptor interaction such as APC co-stimulation, CCR, inflammation-promoting, T cell co-stimulation were higher in the high-risk group, while the Check-point showed significant means (p < 0.05, Fig. 7D).

Discussion

Although some previous studies have shown that several m7G genes may regulate the occurrence and development of KIRC[13–15], the specific mechanism between them is still unknown to a great extent. In this study, we studied the mRNA levels of 29 recently known m7G genes and related survival relationships in human kidney and found that 13/29 (44.8%) genes were differentially expressed surprisingly. In univariate Cox regression analysis, the survival rate was significantly different. These results markedly showed the potential role of m7G in kidney renal clear cell carcinoma and the probability of using these m7G-related genes to establish a prognostic model.

The prediction model proposed in this study consists of 9 m7G-related genes (EIF4A1

EIF4E, GEMIN5, IFIT5, METTL1, NUDT11, NUDT16, NUDT4, WDR4), which can be used to predict the presence of KIRC patients. These genes can be approximately divided into four categories, including those involved in mRNA maturation (EIF4A1, EIF4E, GEMIN5), tRNA processing and gene expression (METTL1, WDR4), metabolic process (NUDT11, NUDT16, NUDT4) and immune response (IFIT5). EIF4A1 and EIF4E belong to the same family of eukaryotic translation initiation factors. Diseases related to EIF4A1 include ovarian sarcoma and late-onset Parkinson's disease. It has been reported that EIF4A1 participates in the interaction of KANK2 / KIF21A, resulting in renal filtration dysfunction[16]. EIF4E plays an important role in KIRC by enhancing immune response to increase chemotherapy effect and reduce recurrence[17, 18]. GEMIN5, this gene encodes WD repeat protein, which is a component of motor neuron (SMN) complex survival[19]. The imbalance of this gene may play a role in mRNA alternative splicing and

tumor cell movement[20, 21]. In terms of tRNA processing and gene expression, METTL1 mainly plays a role in diseases through m7G methylation[22]. It can be used as a tumor suppressor gene in colon cancer, high expression of METTL1 is related to the development and prognosis of liver cancer and bladder cancer[23–25], WDR4 can be used as a good biomarker in liver cancer and lung cancer[26, 27]. Its loss will affect the process of RNA transcription and lead to genetic diseases, Braun has found that it is related to Down syndrome. Lin et al confirmed that WDR4 plays a key role in normal mRNA translation and differentiation[28, 29]. Similarly, NUDT11, NUDT16 and NUDT4 belong to a subclass of Phosphohydrolases. They tend to preferentially attack diphosphate polyphosphate in the body[30]. Some of these genes have been studied, inhibiting the expression of NUDT11 affects the phenotype of cells in prostate cancer, and the lack of NUDT16 leads to DNA damage and development stagnation[31, 32]. however how to play a role in KIRC and its mechanism are unclear, which will be the focus of our next research. IFIT5 (interferon inducible protein and tetratripeptide repeat 5) is a protein coding gene. Interferon induced RNA binding protein is involved in human innate immune response, and its abnormal expression can lead to related diseases, including lice infection[33]. It plays an important role in immunity and signal transduction[34, 35]. Whether these genes act through m7G methylation and affect the prognosis of KIRC patients remains to be clarified.

Based on different types of DEGs in the risk group, we conducted GO and KEGG analysis. Only cellular component (CC) has shown meaningful results in R, the results of cell composition (CC) showed that these genes were mainly involved in the synaptic membrane. Tumor migration and invasion may develop through this pathway. To get Kyoto Encyclopedia of Genes and Genomes (KEGG) pathways analysis, online KOBAS database of top ten genes in DEGs showed that the genes are mainly related to Immune dysfunction. Tumor immunotherapy is a hot spot in tumor therapy, which is widely used in the research and treatment of KIRC[36]. The immune infiltration of tumor cells and lymph node metastasis are closely related to the prognosis of cancer. We compared the level of infiltrating immune cells and immune function between high-risk and low-risk. From the differential genes of TCGA, we found that the immune function at high-risk was fully inhibited. T cells and pDCs cells are important immune cells in the body and have a wide range of anti-tumor effects[37, 38]. Enhancement of T cells in lung cancer can block the signal pathway of transforming growth factor T and play an anti-tumor role[39]. The possible reason is that the abnormal expression of m7G methylation leads to the change of mRNA in the process of transcriptional modification, which affects its function and leads to immune dysfunction. In addition, the high-risk group may be related to the impairment of anti-tumor immunity. The activity of type II interferon response, type I interferon response and the activation of immune factors play an important role in anti-tumor. There is no significant difference between the high-risk group and the low-risk group in this study. Therefore, the weakening of antitumor immunity in high-risk patients may be the key to their poor prognosis, but the mechanism needs to be further studied.

However, there are some unavoidable defects in our research. Firstly, our data only comes from the database TCGA, which includes some incomplete data. We need more and larger sample size to verify our results. Second, the molecular mechanism of immunity needs more experimental such as western

blotting and prospective studies to explore and testify our results. We believe that experimental research will help to verify these results in the future.

In conclusion, we found that m7G methylation was associated with tumor development in KIRC patients. Our study confirmed 9 differential genes related to prognosis. Besides, the risk scores and levels of nine m7G-related genes generated according to our risk model are independent risk factors for predicting OS. DEGs between high-risk group and low-risk group are related to tumor immunity. This study provides a new gene marker for the prognosis of KIRC patients and an important basis for the study of the relationship between KIRC m7G-related genes and immunity.

Declarations

DATA AVAILABILITY STATEMENT

All available data were analyzed in this study. These can be found here: TCGA (https://portal.gdc.cancer.gov/), STRING(https://cn.stringdb.org/), R(https://www.r-project.org/), KOBAS (http://kobas.cbi.pku.edu.cn/kobas3/genelist/).

ETHICS STATEMENT

Ethical review and approval were not required for the study on human participants in accordance with the local legislation and institutional requirements. Written informed consent for participation was not required for this study in accordance with the national legislation and the institutional requirements.

FUNDING

This research was supported by the Natural Science Foundation of Jiangxi Provincial [20171BAB205064].

AUTHOR CONTRIBUTIONS

LB, FC wrote the paper. ZW edited the paper. All authors contributed to the article and approved the submitted version. All authors have no related financial or non-financial conflicts of interest.

Acknowledgments

We acknowledge the TCGA, STRING, R and other tools for free use.

References

1. Siegel, R.L., K.D. Miller, and A. Jemal, *Cancer statistics, 2019*. CA Cancer J Clin, 2019. **69**(1): p. 7–34.
2. Sun, Z., et al., *Comprehensive Analysis of the Immune Infiltrates of Pyroptosis in Kidney Renal Clear Cell Carcinoma*. Front Oncol, 2021. **11**: p. 716854.

3. Méjean, A., et al., *Sunitinib Alone or after Nephrectomy in Metastatic Renal-Cell Carcinoma*. N Engl J Med, 2018. **379**(5): p. 417–427.
4. Inman, B.A., M.R. Harrison, and D.J. George, *Novel immunotherapeutic strategies in development for renal cell carcinoma*. Eur Urol, 2013. **63**(5): p. 881–9.
5. Jones, P.A., *Functions of DNA methylation: islands, start sites, gene bodies and beyond*. Nat Rev Genet, 2012. **13**(7): p. 484–92.
6. Lin, G., et al., *Hub Long Noncoding RNAs with m6A Modification for Signatures and Prognostic Values in Kidney Renal Clear Cell Carcinoma*. Front Mol Biosci, 2021. **8**: p. 682471.
7. Zhang, C., et al., *Downregulated METTL14 accumulates BPTF that reinforces super-enhancers and distal lung metastasis via glycolytic reprogramming in renal cell carcinoma*. Theranostics, 2021. **11**(8): p. 3676–3693.
8. Tomikawa, C., *7-Methylguanosine Modifications in Transfer RNA (tRNA)*. Int J Mol Sci, 2018. **19**(12).
9. Colaprico, A., et al., *TCGAbiolinks: an R/Bioconductor package for integrative analysis of TCGA data*. Nucleic Acids Res, 2016. **44**(8): p. e71.
10. Ritchie, M.E., et al., *limma powers differential expression analyses for RNA-sequencing and microarray studies*. Nucleic Acids Res, 2015. **43**(7): p. e47.
11. Chen, H. and P.C. Boutros, *VennDiagram: a package for the generation of highly-customizable Venn and Euler diagrams in R*. BMC Bioinformatics, 2011. **12**: p. 35.
12. Simon, N., et al., *Regularization Paths for Cox's Proportional Hazards Model via Coordinate Descent*. J Stat Softw, 2011. **39**(5): p. 1–13.
13. Jacobson, M.R. and T. Pederson, *A 7-methylguanosine cap commits U3 and U8 small nuclear RNAs to the nucleolar localization pathway*. Nucleic Acids Res, 1998. **26**(3): p. 756–60.
14. Lin, S. and S. Ohno, *The interactions of androgen receptor with poly(A)-containing RNA and polyribonucleotides*. Eur J Biochem, 1982. **124**(2): p. 283–7.
15. Furuse, Y., *RNA Modifications in Genomic RNA of Influenza A Virus and the Relationship between RNA Modifications and Viral Infection*. Int J Mol Sci, 2021. **22**(17).
16. Xu, Y., et al., *Nephrotic-syndrome-associated mutation of KANK2 induces pathologic binding competition with physiological interactor KIF21A*. J Biol Chem, 2021. **297**(2): p. 100958.
17. Cao, J., et al., *Inhibition of eIF4E cooperates with chemotherapy and immunotherapy in renal cell carcinoma*. Clin Transl Oncol, 2018. **20**(6): p. 761–767.
18. Das, F., et al., *TGFβ-induced PI 3 kinase-dependent Mnk-1 activation is necessary for Ser-209 phosphorylation of eIF4E and mesangial cell hypertrophy*. J Cell Physiol, 2013. **228**(7): p. 1617–26.
19. Martinez-Salas, E., A. Embarc-Buh, and R. Francisco-Velilla, *Emerging Roles of Gemin5: From snRNPs Assembly to Translation Control*. Int J Mol Sci, 2020. **21**(11).
20. Gabanella, F., et al., *Ribonucleoprotein assembly defects correlate with spinal muscular atrophy severity and preferentially affect a subset of spliceosomal snRNPs*. PLoS One, 2007. **2**(9): p. e921.

21. Kour, S., et al., *Loss of function mutations in GEMIN5 cause a neurodevelopmental disorder*. Nat Commun, 2021. **12**(1): p. 2558.
22. Pandolfini, L., et al., *METTL1 Promotes let-7 MicroRNA Processing via m7G Methylation*. Mol Cell, 2019. **74**(6): p. 1278–1290.e9.
23. Tian, Q.H., et al., *METTL1 overexpression is correlated with poor prognosis and promotes hepatocellular carcinoma via PTEN*. J Mol Med (Berl), 2019. **97**(11): p. 1535–1545.
24. Liu, Y., et al., *Methyltransferase-like 1 (METTL1) served as a tumor suppressor in colon cancer by activating 7-methyguanosine (m7G) regulated let-7e miRNA/HMGA2 axis*. Life Sci, 2020. **249**: p. 117480.
25. Ying, X., et al., *METTL1-m(7) G-EGFR/EFEMP1 axis promotes the bladder cancer development*. Clin Transl Med, 2021. **11**(12): p. e675.
26. Xia, P., et al., *MYC-targeted WDR4 promotes proliferation, metastasis, and sorafenib resistance by inducing CCNB1 translation in hepatocellular carcinoma*. Cell Death Dis, 2021. **12**(7): p. 691.
27. Ma, J., et al., *METTL1/WDR4-mediated m(7)G tRNA modifications and m(7)G codon usage promote mRNA translation and lung cancer progression*. Mol Ther, 2021. **29**(12): p. 3422–3435.
28. Braun, D.A., et al., *Mutations in WDR4 as a new cause of Galloway-Mowat syndrome*. Am J Med Genet A, 2018. **176**(11): p. 2460–2465.
29. Lin, S., et al., *Mettl1/Wdr4-Mediated m(7)G tRNA Methylome Is Required for Normal mRNA Translation and Embryonic Stem Cell Self-Renewal and Differentiation*. Mol Cell, 2018. **71**(2): p. 244–255.e5.
30. Hua, L.V., et al., *Paralogous murine Nudt10 and Nudt11 genes have differential expression patterns but encode identical proteins that are physiologically competent diphosphoinositol polyphosphate phosphohydrolases*. Biochem J, 2003. **373**(Pt 1): p. 81–9.
31. Iyama, T., et al., *NUDT16 is a (deoxy)inosine diphosphatase, and its deficiency induces accumulation of single-strand breaks in nuclear DNA and growth arrest*. Nucleic Acids Res, 2010. **38**(14): p. 4834–43.
32. Grisanzio, C., et al., *Genetic and functional analyses implicate the NUDT11, HNF1B, and SLC22A3 genes in prostate cancer pathogenesis*. Proc Natl Acad Sci U S A, 2012. **109**(28): p. 11252–7.
33. Pidugu, V.K., et al., *Emerging Functions of Human IFIT Proteins in Cancer*. Front Mol Biosci, 2019. **6**: p. 148.
34. Lo, U.G., et al., *IFNγ-Induced IFIT5 Promotes Epithelial-to-Mesenchymal Transition in Prostate Cancer via miRNA Processing*. Cancer Res, 2019. **79**(6): p. 1098–1112.
35. Wu, X., et al., *Duck IFIT5 differentially regulates Tembusu virus replication and inhibits virus-triggered innate immune response*. Cytokine, 2020. **133**: p. 155161.
36. Liu, X.S., et al., *NPM1 Is a Prognostic Biomarker Involved in Immune Infiltration of Lung Adenocarcinoma and Associated With m6A Modification and Glycolysis*. Front Immunol, 2021. **12**: p. 724741.

37. Bruno, T.C., *New predictors for immunotherapy responses sharpen our view of the tumour microenvironment*. Nature, 2020. **577**(7791): p. 474–476.
38. Shevtsov, M. and G. Multhoff, *Immunological and Translational Aspects of NK Cell-Based Antitumor Immunotherapies*. Front Immunol, 2016. **7**: p. 492.
39. Germain, C., et al., *Presence of B cells in tertiary lymphoid structures is associated with a protective immunity in patients with lung cancer*. Am J Respir Crit Care Med, 2014. **189**(7): p. 832–44.

Figures

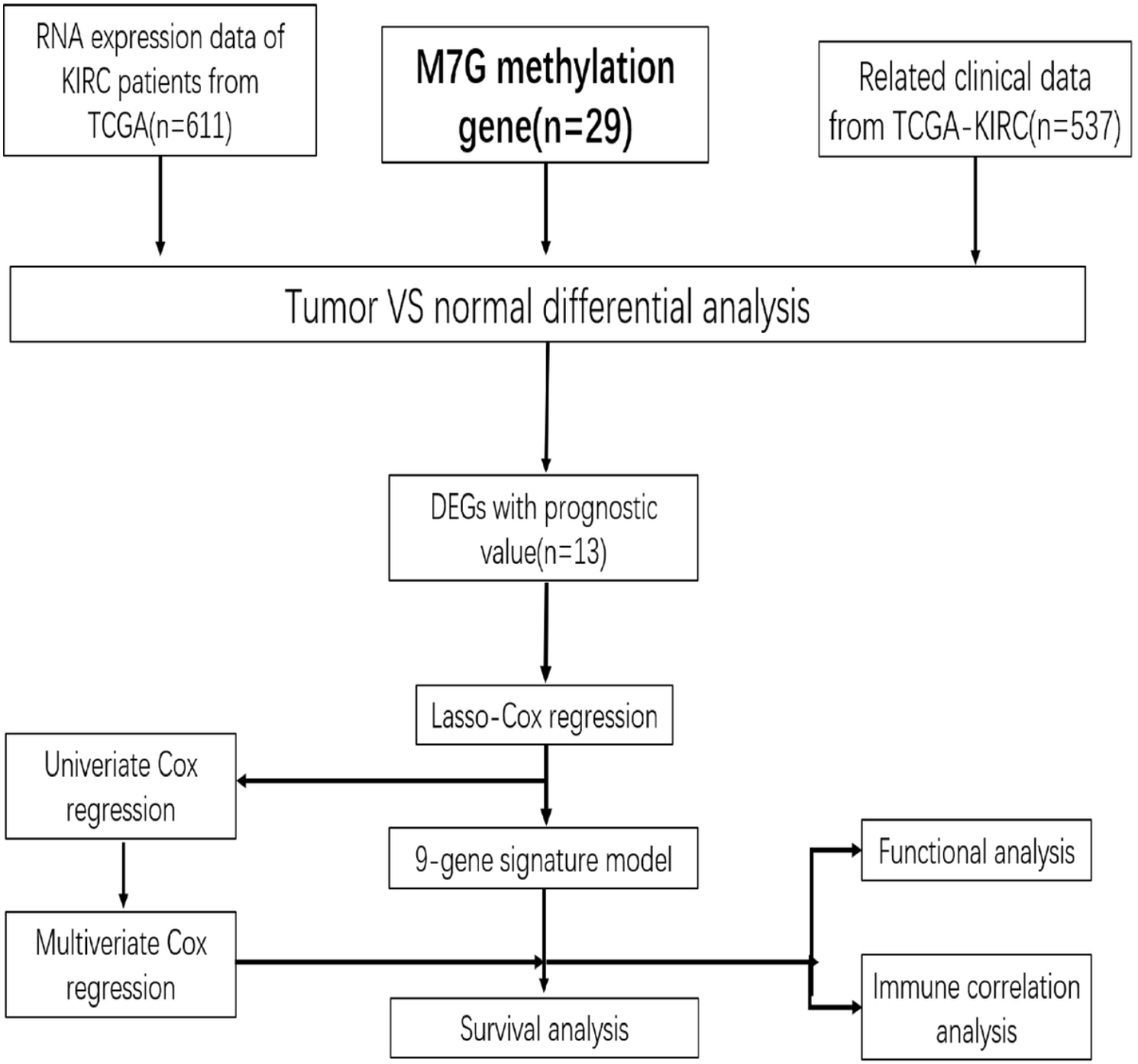

Figure 1

The research design and workflow of this paper

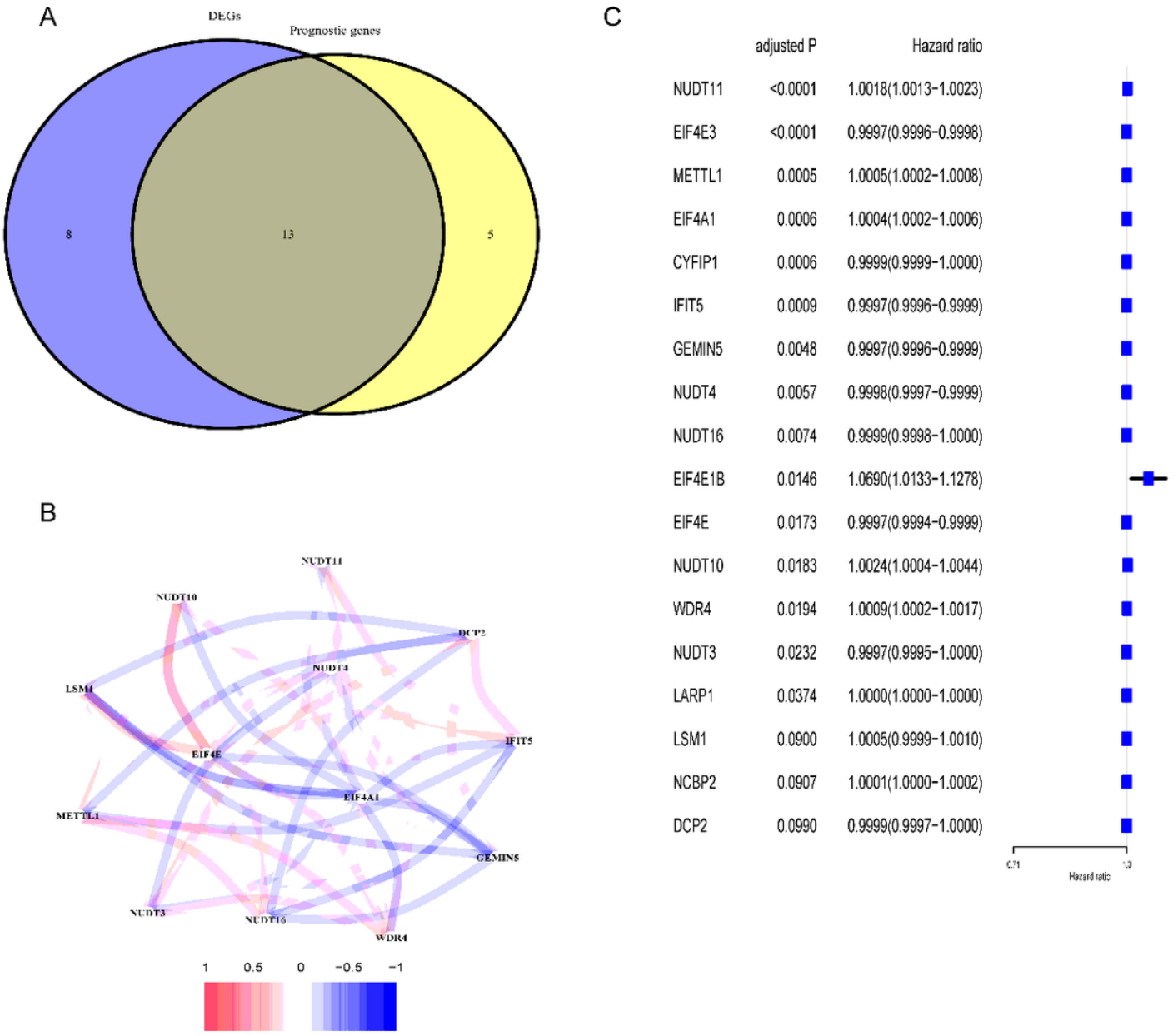

Figure 2

A. Venn map was used to determine the differentially expressed genes related to m7G between tumor and adjacent normal tissues; B. The correlation network of 13 candidate genes; C. Forest map of univariate analysis results of prognostic genes(p<0.1).

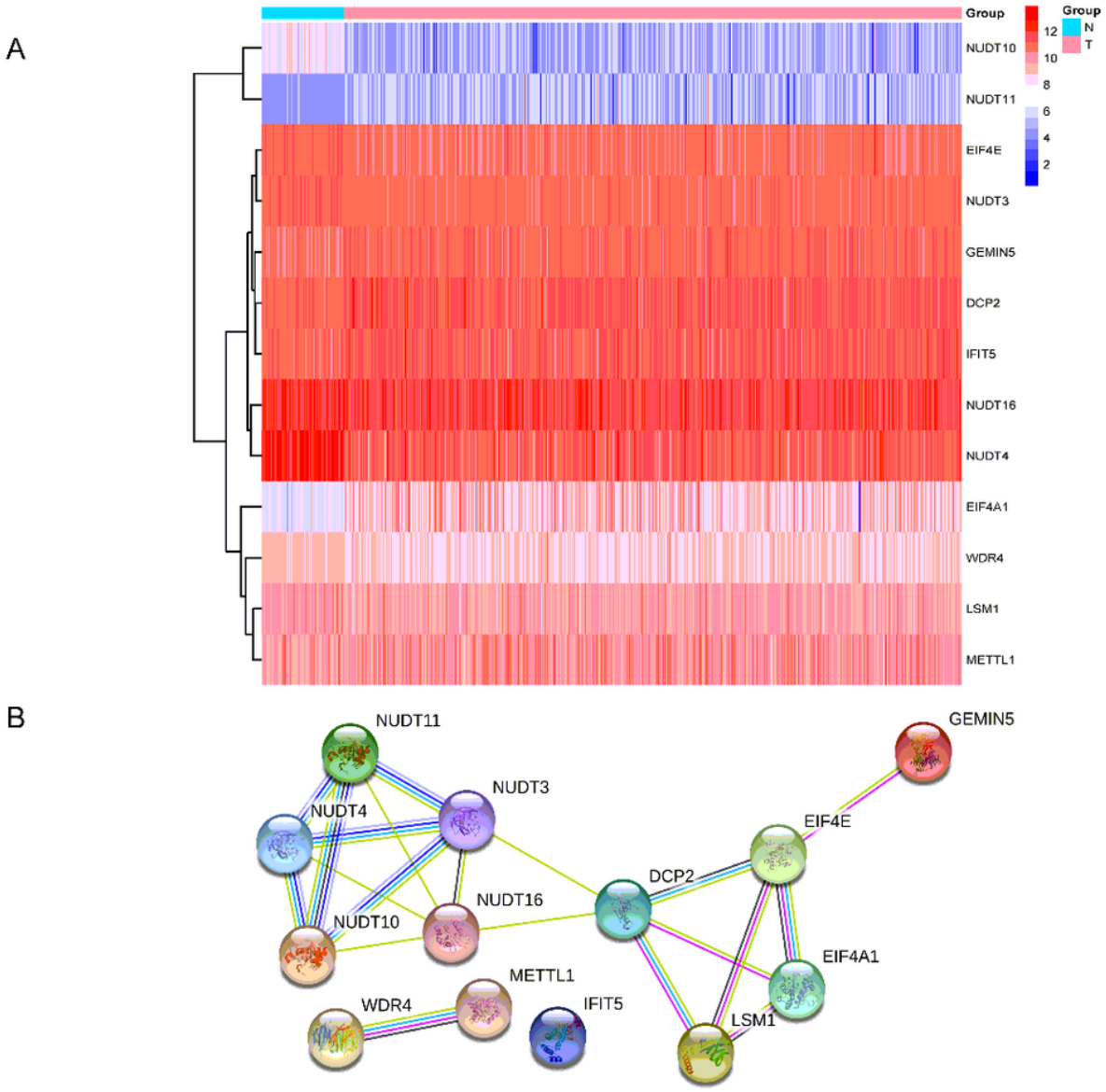

Figure 3

A. Heat map of 13 overlapping genes in tumor tissue. B. The PPI network downloaded from the STRING database indicates the interaction between candidate genes

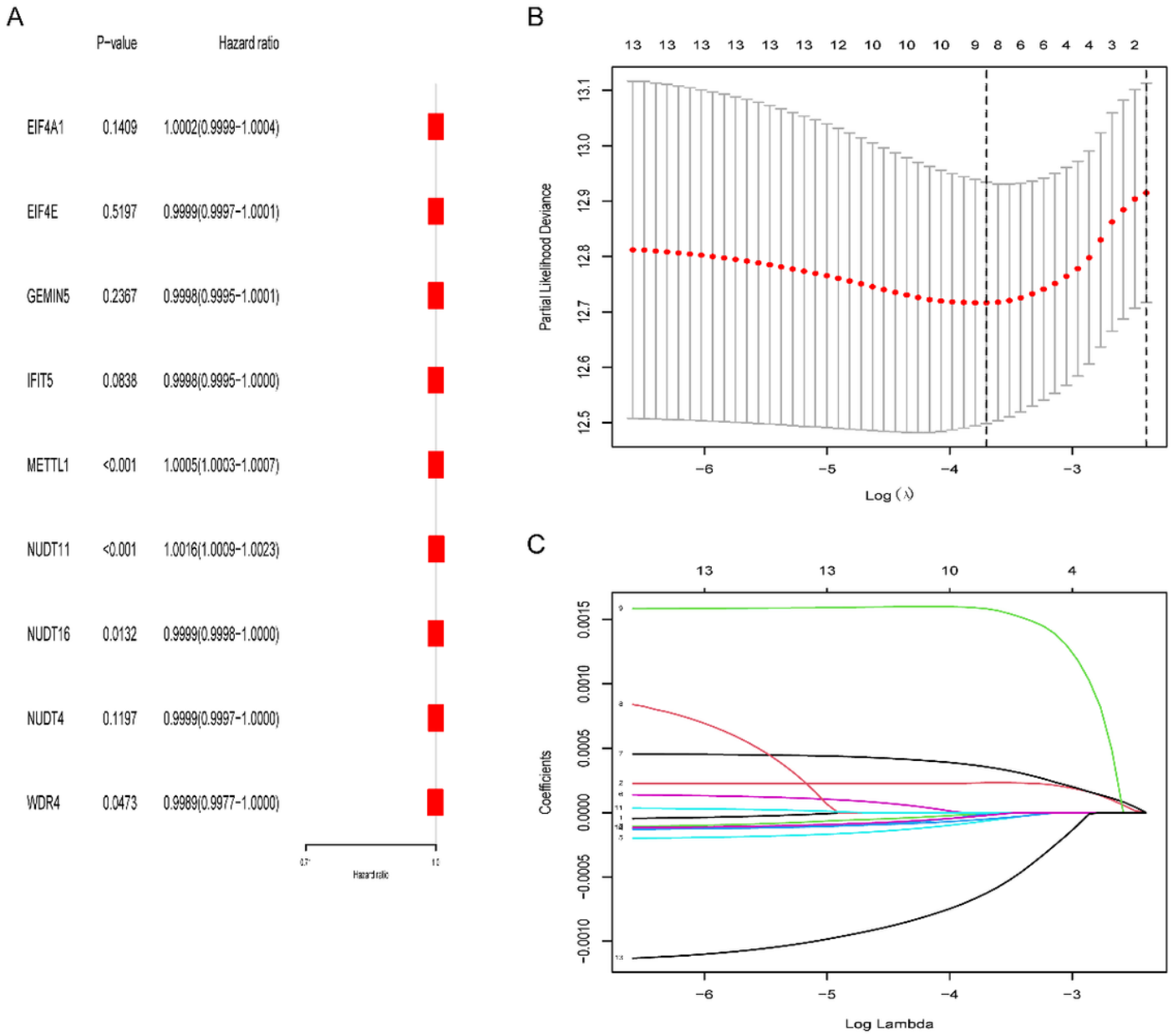

Figure 4

Construction of risk characteristics in TCGA. (A) Univariate Cox regression analysis of OS for 9 m7G-related genes;(B) LASSO regression of the 9 OS-related genes;(C) Cross validation is used to adjust the parameter selection in LASSO regression.

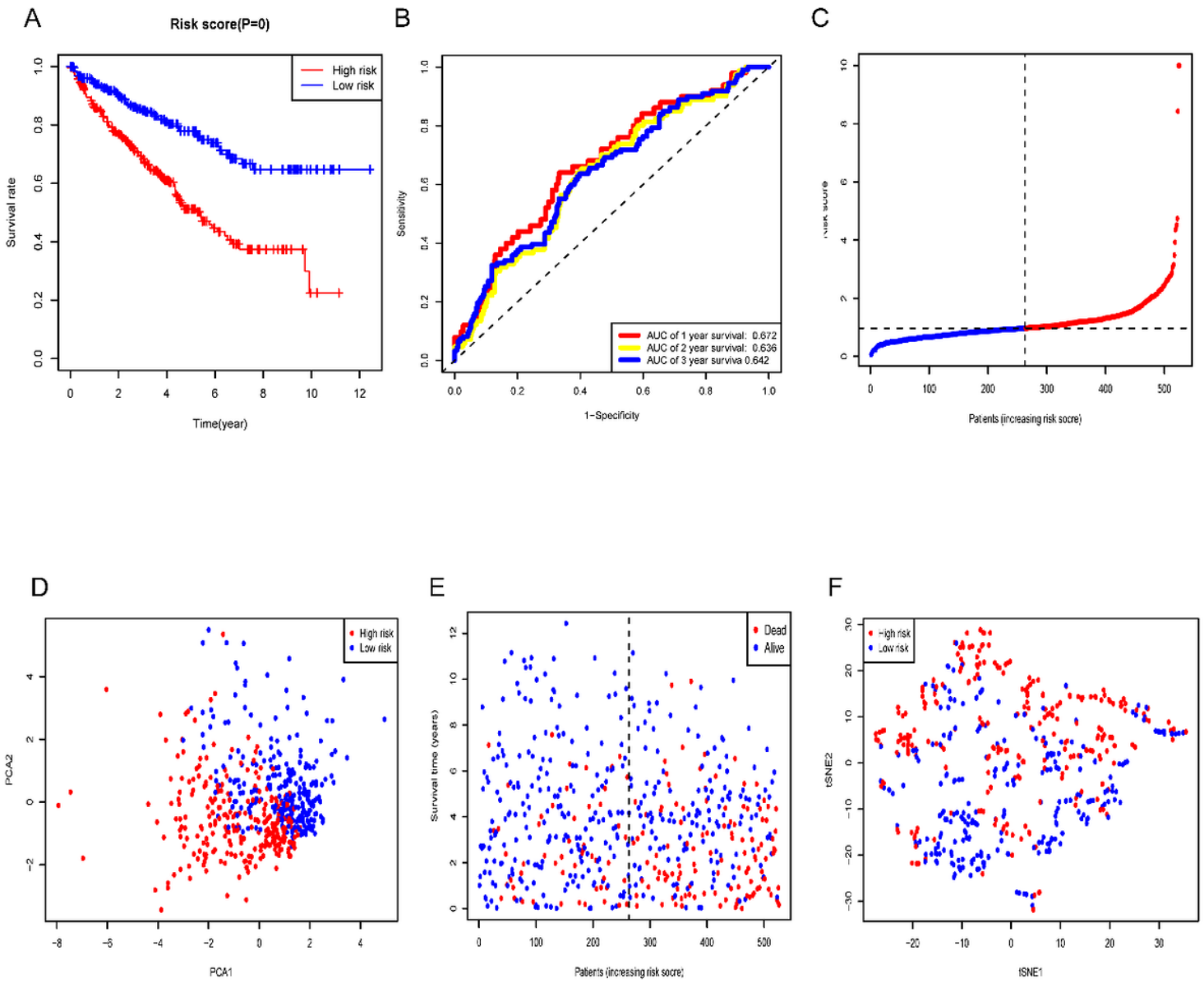

Figure 5

A. Kaplan Meier OS curve of patients in high-risk group and low-risk group; B. The ROC curve shows the prediction efficiency of risk score; C. Distribution of patients based on the risk score; D. PCA plot for KIRC based on the risk score; E. Survival status of each patient; F. t-SNE plot for KIRC based on the risk score.

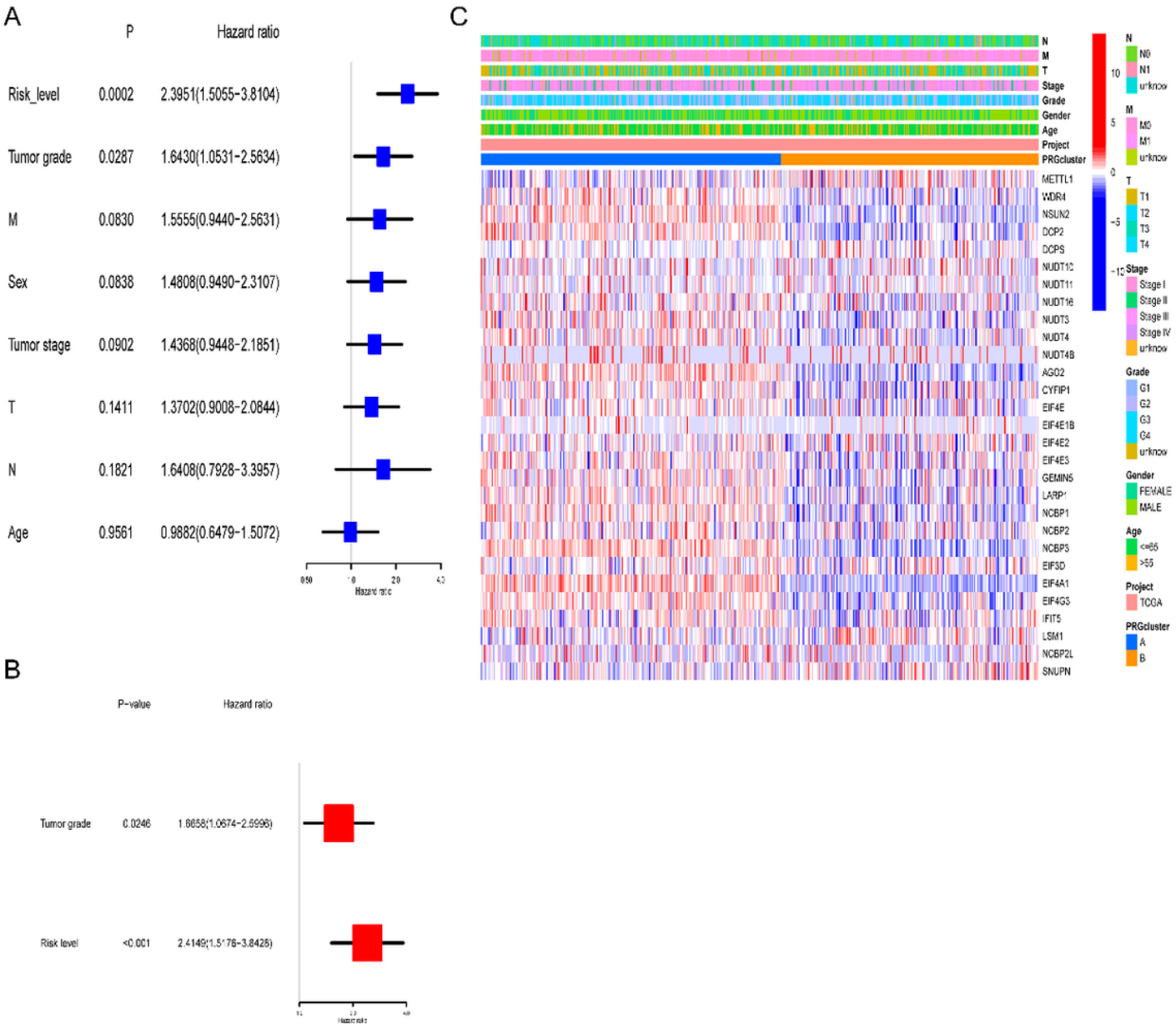

Figure 6

Univariate and multivariate Cox regression analysis of risk score. (A) Univariate analysis for the TCGA cohort;(B) Multivariate analysis for the TCGA cohort; (C) Heatmap of the association between clinicopathological features and risk groups.

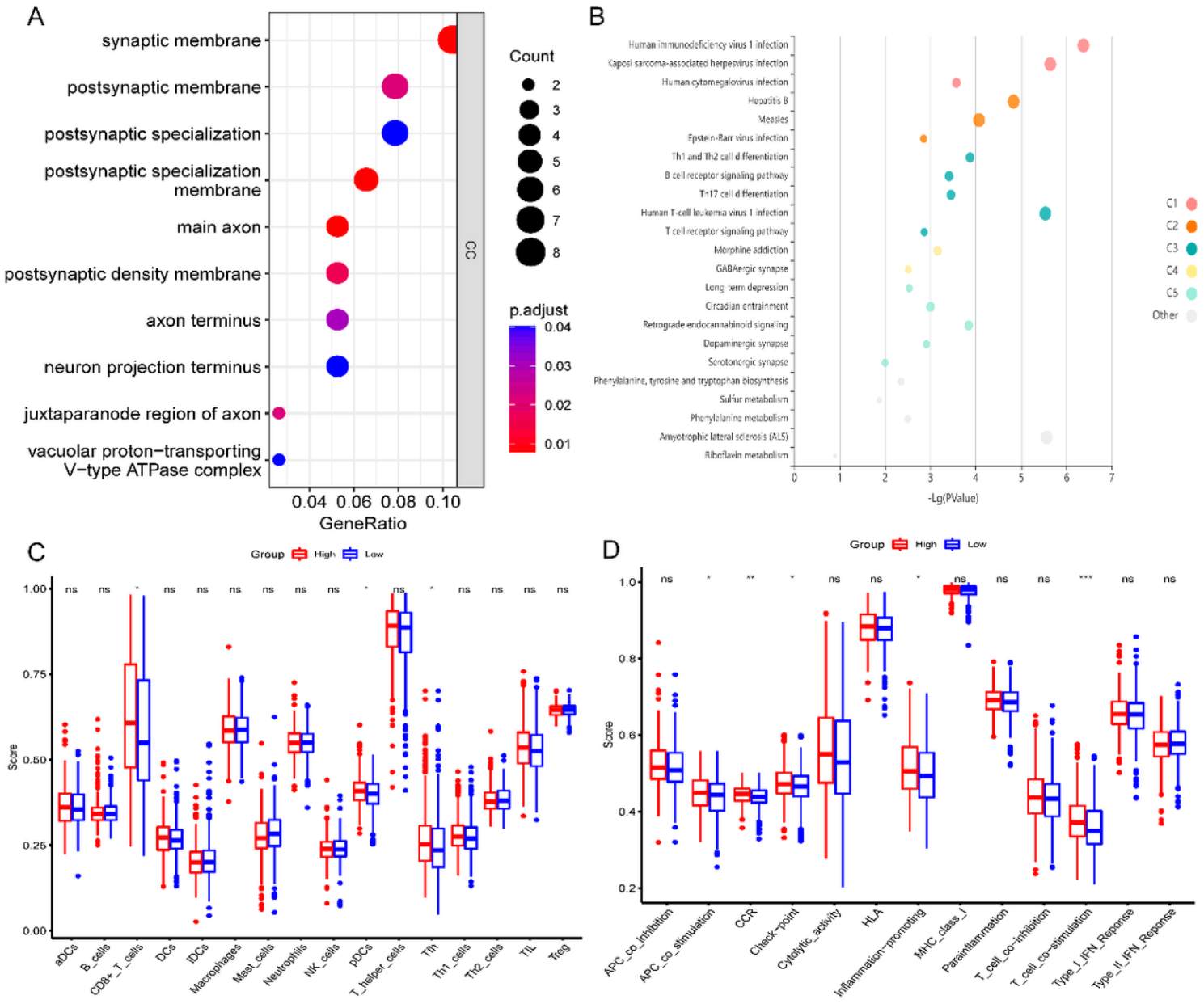

Figure 7

A. The most significant or shared GO enrichment in the TCGA cohort is displayed; B. Bubble Diagram of KEGG pathways (the bigger bubble means the more genes enriched, and the increasing depth of red means the differences were more obvious; q-value: the adjusted p-value). C and D. Comparison of ssGSEA scores of immune cells and immune pathways (Comparison of the tumor immunity between low- and high-risk group in the TCGA. *P < 0.05; **P< 0.01; ***P < 0.001).

Supplementary Files

This is a list of supplementary files associated with this preprint. Click to download.

- SupplementTable1m7Ggene.docx